Coherent Ultrashort Light Pulse Code-Division Multiple Access Communication Systems

JAWAD A. SALEHI, MEMBER, IEEE, ANDREW M. WEINER, AND JONATHAN P. HERITAGE, SENIOR MEMBER, IEEE

Abstract—**We analyze a new technique for encoding and decoding of coherent ultrashort light pulses. In particular, we discuss the temporal and statistical behavior of pseudonoise bursts generated by spectral phase coding of ultrashort optical pulses. Our analysis is motivated by recent experiments that demonstrate high resolution spectral phase coding of picosecond and femtosecond pulses and suggest the possibility of ultrahigh speed code-division multiple access (CDMA) communications using this technique. We trace the evolution of coherent ultrashort pulses into low intensity pseudonoise bursts as a function of the degree of phase coding. For random coding we find that the encoded pulse obeys Gaussian statistics and that the intensity probability distribution function is a negative exponential. These results are utilized to analyze the performance of a proposed CDMA optical communications system based upon encoding and decoding of ultrashort light pulses. We derive the bit error rate (BER) as a function of data rate, number of users, and receiver threshold; and we discuss the performance characteristics for a variety of system parameters. We find that performance improves dramatically with increasing code length. Ultrashort light pulse CDMA could provide tens to hundreds of users with asynchronously multiplexed, random access to a common optical channel.**

I. INTRODUCTION

DUE TO ECONOMIC advantages, maturing technology, and high information capacity, single-mode fiber-optic transmission media will be embedded in future telecommunications networks. A desirable feature for these future optical networks would be the ability to process information directly in the optical domain for purposes of multiplexing, demultiplexing, filtering, amplification, and correlation. Optical signal processing would be advantageous because potentially it can be much faster than electrical signal processing and because it would obviate the need for photon–electron–photon conversions. Several new classes of optical networks are now emerging [1]. For example, code-division multiple access (CDMA) networks using optical signal processing techniques were recently introduced [2]–[9]. CDMA is a type of spread spectrum communications [10] in which multiplexing is achieved by assigning different, minimally interfering code sequences to different user pairs. In fiber optic CDMA, users communicate by imprinting their message bits upon their own unique code, which they transmit asynchronously (with respect to the other transmitters) over a common channel. A matched filter at the receiver end ensures that data are detected only when they are imprinted on the proper code sequence (see Fig. 1). This approach to multiplexing allows transmission without delay and handles multiaccess interference (contention) as an integral part of the multiplexing scheme.

In this paper we analyze a novel ultrashort pulse optical CDMA network. Our analysis is motivated by recent experiments which demonstrate encoding and decoding of femtosecond pulses and which suggest the possibility of ultrahigh speed CDMA communications using this technique [8], [9]. We first examine the temporal and statistical behavior of pseudonoise bursts generated by spectral phase coding of ultrashort optical pulses. Then, we apply the statistical results derived here to perform a bit error rate analysis of the proposed ultrashort pulse CDMA system.

Before beginning the analysis, we first summarize the experimental results on encoding and decoding of ultrashort pulses and review the proposed scheme for ultrashort pulse CDMA, shown schematically in Fig. 2. In the transmitter a coherent ultrashort pulse representing one bit of information is directed to the optical encoder, which consists of a pair of diffraction gratings placed at the focal planes of a unit magnification, confocal lens pair. This apparatus was previously utilized for high resolution, temporal shaping of coherent ultrashort pulses [11]–[14]. The first grating spatially decomposes (with a certain resolution) the spectral components which constitute the input ultrashort pulse. A pseudorandom, spatially patterned phase mask is inserted midway between the lenses at the point where the optical spectral components experience maximal spatial separation. Thus, the mask introduces pseudorandom phase shifts (address codes) among the different spectral components. After the phase mask, the spectral components are reassembled by the second lens and second grating into a single optical beam. After emerging from the grating and lens apparatus, the temporal profile of the encoded pulse is given by the Fourier transform of the pattern transferred by the mask onto the spectrum. A pseudorandom phase mask transforms the incident ultrashort pulse into a low intensity pseudonoise burst.

In the CDMA network, each transmitter has a distinct phase mask and broadcasts its encoded pulses to all those receivers that share the same optical channel. A receiver consists of a decoder and an optical threshold device. The

Manuscript received April 14, 1989; revised August 28, 1989. This paper was presented in part at the 1988 International Symposium on Information Theory and the 1989 International Conference on Communications.

The authors are with Bellcore, Morristown, NJ 07960-1961.

IEEE Log Number 8932059.

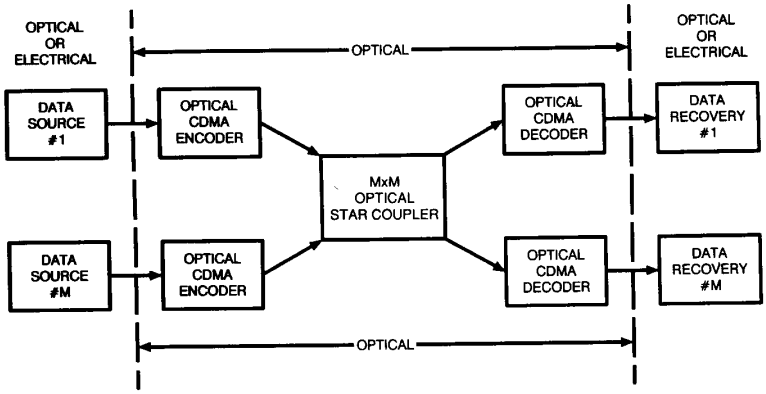

Fig. 1. A schematic diagram of an optical code division multiple-access communications system with an all-optical encoder and decoder.

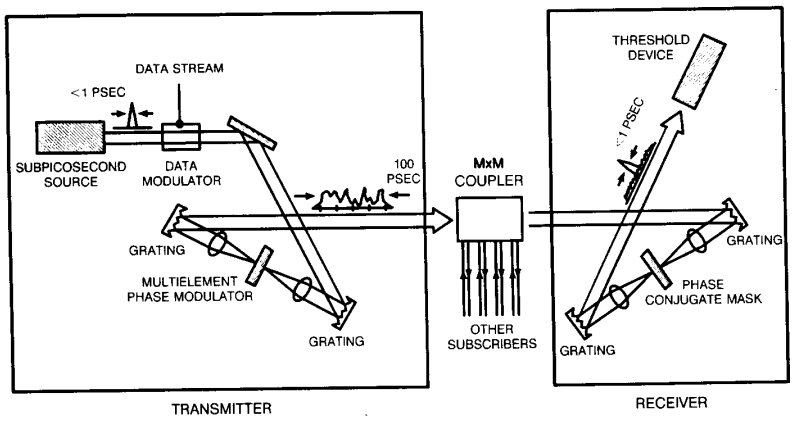

Fig. 2. Proposed scheme for optical CDMA based on spectral encoding and decoding of ultrashort light pulses. Only one transmitter station and one receiver station are shown.

optical decoder is similar to the optical encoder except that its phase mask is the conjugate of the encoding mask. Thus a pulse is properly decoded when the encoding and decoding masks are a complex conjugate pair. In this case the spectral phase shifts are removed and the original coherent ultrashort pulse is reconstructed. On the other hand, when the encoding and decoding masks do not match, the spectral phase shifts are rearranged but not removed, and the pulse at the output of the decoder remains a low intensity pseudonoise burst. The threshold device is set to detect data corresponding to intense, properly decoded pulses and to reject low intensity, improperly decoded, pseudonoise bursts.

We now illustrate encoding and decoding by referring to an experiment in which 75-fs optical pulses were encoded by using a 44-element pseudorandom binary phase mask [9]. Fig. 3(a) depicts an intensity autocorrelation measurement of the incident, uncoded pulses together with that of the encoded pulses. The contrast ratio of $\simeq 25:1$ illustrates the dramatic reduction in intensity that accompanies encoding. In order to demonstrate decoding, a second phase mask was placed adjacent to the first mask.

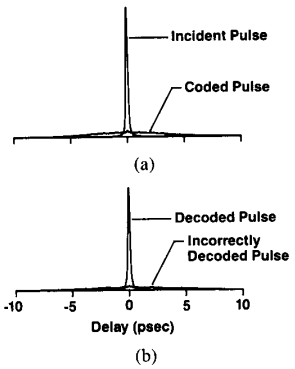

Fig. 3. Experimental intensity autocorrelation measurements of uncoded, coded, and decoded pulses, from [9]. (a) The uncoded, incident pulse and an encoded pulse. (b) Successfully and unsuccessfully decoded pulses.

When the second mask is phase-conjugate to the first, decoding is successful, and the initial pulse is restored. When the second mask does not match the first, decoding is unsuccessful and low intensity, pseudonoise behavior

is retained. Intensity autocorrelation measurements of such successfully and unsuccessfully decoded pulses, shown in Fig. 3(b), exhibit a contrast similar to that observed for encoding alone. Encoding and decoding was subsequently demonstrated for longer codes composed of 127 elements; and using 1-in optics, encoding should theoretically be possible for code lengths as high as 2000 [14].

At this point we comment on the effect of the transmission channel in the proposed ultrashort pulse CDMA system. Although so far we have implicitly assumed that the phases spectrally encoded onto the input pulse remain intact after transmission, any real CDMA network must transport encoded pulses to a plurality of potential users while maintaining the integrity of the code. Any transmission medium except the vacuum is dispersive and potentially nonlinear, and both effects can significantly distort an ultrashort pulse. One possible CDMA configuration which completely avoids these difficulties would employ free space optical interconnects. Such a configuration, which might occupy a small optical platform, would serve as a multiple access switch at a node in a larger network of more conventional design. Of course, in order to construct a pure ultrashort pulse CDMA network connecting remote locations, single-mode optical fibers will be required, and dispersion will place a limit on the maximum practical fiber length. Fortunately, in the low power limit where nonlinear effects are negligible, the grating configuration that is used for coding and decoding can also be used to pre- or post-compensate for fiber dispersion [15]. Recent calculations show [16] that a 0.3-ps pulse tuned close to the zero-dispersion wavelength can propagate up to 10 km in a single mode fiber and still be recovered with minimum distortion by grating compensation. Therefore, we expect that fiber dispersion need not be a serious problem for an ultrashort pulse CDMA system. In our analysis we will assume that any effects due to dispersion or nonlinearity of the transmission channel can be safely neglected.

It is the purpose of our analysis to determine the bit error rate (BER) of an ultrashort pulse CDMA system as described above. To obtain the BER, it is first necessary to investigate the statistics of interference at the receiver due to improperly decoded signals. In this paper we first look at the temporal and statistical properties of encoded (or unsuccessfully decoded) pulses from a single user. We extend these results to the case of a varying (statistical) number of interfering improperly decoded pulses and derive the BER as a function of various system parameters, such as the number of users, the individual bit rates, the threshold, and the length of the codes.

In Section II of this paper we discuss statistically the effect of random coding on a band-limited optical pulse. Furthermore, we compare the effect of different levels of coding using computer simulation techniques. We show that under random encoding the pulse feature completely disappears and a low intensity background noise appears.

In Section III we study the first and second degree of coherence (the field and intensity autocorrelation functions) for an encoded pulse and highlight some striking similarities that exist between the randomly encoded pulse and the output of a typical free-running multimode laser.

In Section IV we study the probability distribution function for the pseudonoise bursts produced by encoding and discuss the conditions under which pseudonoise bursts behave like random light. In particular, for a randomly encoded pulse with a random initial phase and transmission time, the statistics are modeled as Gaussian and the intensity probability distribution function is a negative exponential.

In Section V we derive the bit error rate (BER) as a function of data rate, code length, number of users, and receiver threshold; and we discuss the performance characteristics for a variety of system parameters.

We conclude this paper in Section VI. The Appendix is devoted to detailed mathematical analyses that are needed to support the results of Section V.

II. Statistical Analysis of Encoded Ultrashort Light Pulses

We now analyze the statistics of single encoded pulses. We assume that the starting ultrashort pulses are characterized by a baseband Fourier spectrum $A(\omega)$ given by

$$A(\omega) = \begin{cases} \dfrac{\sqrt{P_0}}{W}, & \text{for } \dfrac{-W}{2} \le w \le \dfrac{W}{2} \\ 0, & \text{elsewhere} \end{cases} \tag{1}$$

where P_0 is the peak power of the ultrashort pulse and W is the total bandwidth of the band-limited source. The temporal pulse shape $a(t)$ is a sinc function:

$$a(t) = \sqrt{P_0}\ \text{sinc}\left(\frac{W}{2}t\right) \tag{2}$$

where sinc $(x) = \sin x/x$. The field amplitude $a(t)$ is normalized so that $|a(t)|^2$ gives the instantaneous power $P(t)$, whence

$$P(t) = P_0\ \text{sinc}^2\left(\frac{W}{2}t\right). \tag{3}$$

Equation (3) describes an isolated ultrashort light pulse with a duration τ_c inversely proportional to the bandwidth of the band-limited source, i.e., $\tau_c \simeq (2\pi/W)$.

To encode a pulse we multiply the starting spectrum $A(\omega)$ by a phase mask consisting of N_0 distinct chips, each of bandwidth $\Omega = (W/N_0)$ (see Fig. 4). The phase of each chip may be adjusted independently; the example given in Fig. 4 shows the special case of a binary phase code. The time domain representation of the encoded field amplitude $C(t)$ can be written as

$$C(t) = \text{sinc}\left(\frac{\Omega}{2}t\right)\frac{\sqrt{P_0}}{N_0}\sum_{n=-N}^{N}\exp\left\{-i(n\Omega t + \varphi_n)\right\}$$
$$= G(t)\,V(t). \tag{4}$$

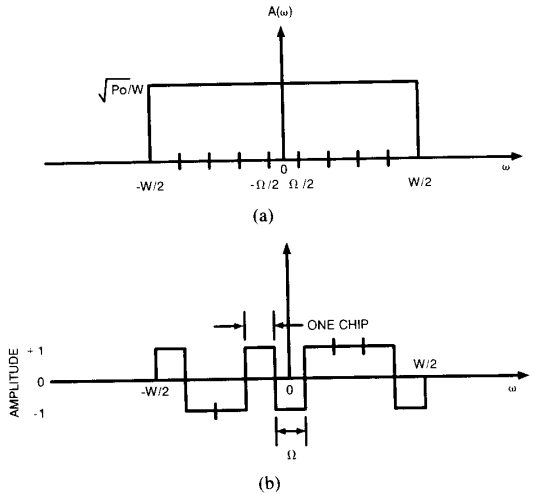

Fig. 4. (a) Spectrum for a band-limited signal, corresponding to an uncoded ultrashort pulse. (b) A typical spectral phase code. An amplitude of +1 corresponds to a phase of 0; an amplitude of −1 corresponds to a phase of π. $W/\Omega = N_0$ is the number of chips in the code.

Here φ_n represents the nth element of a code consisting of $N_0 = 2N + 1$ chips, and

$$G(t) = \operatorname{sinc}\left(\frac{\Omega}{2}t\right) \tag{5}$$

and

$$V(t) = \frac{\sqrt{P_0}}{N_0}\sum_{n=-N}^{N}\exp\left\{-i(n\Omega t + \varphi_n)\right\}. \tag{6}$$

Thus (4) is expressed as the product of two signals $G(t)$ and $V(t)$. The signal $G(t)$ is a real envelope function which determines the temporal width of the encoded pulse and is independent of the code elements. $V(t)$ is a periodic pseudonoise signal with period $T = 2\pi/\Omega$, its temporal shape depends on the code elements φ_n. Note that if $\varphi_n = 0$ for all n, (4) reduces to (2).

In the following we concentrate our attention on the temporal and statistical behavior of the periodic signal $V(t)$. Roughly one period of $V(t)$ fits within the envelope function $G(t)$; hence the encoded signal $C(t)$ corresponds to one period of the periodic signal $V(t)$.

At this point we introduce some notation. The intensity signal $I(t)$ is defined as the square of the periodic part of the encoded signal; $I(t) = |V(t)|^2$. Also we define $V_p(t)$ and $I_p(t)$ as the laser output for the case $\varphi_n = 0$ for all n:

$$V_p(t) = \frac{\sqrt{P_0}}{N_0}\sum_{n=-N}^{N}\exp\left\{-i(n\Omega t)\right\} \tag{7}$$

and

$$I_p(t) = \frac{P_0}{N_0^2}\sum_{n=-N}^{N}\sum_{m=-N}^{N}\exp\left\{-i(n-m)\Omega t\right\}. \tag{8}$$

$V_p(t)$ and $I_p(t)$ represent a periodic train of ultrashort pulses with period T and with a pulse duration (τ_c) inversely proportional to $N_0\Omega$. Thus, we may think of $V_p(t)$ and $I_p(t)$, respectively, as the representations of the field amplitude and the intensity of an ideal mode-locked laser with a pulsation period T, peak power P_0, and without a phase mask. Note that, $a(t) = G(t)\,V_p(t)$ and $P(t) = G^2(t)\,I_p(t)$. Analogously we may think of $V(t)$, with $\varphi_n \neq 0$, as the output of a free-running multimode laser with a period T, and $|C(t)|^2 = G^2(t)\,I(t)$.

Our previously reported encoding and decoding experiments [8], [9] utilized binary phase masks, where the phase of each chip was set to either 0 or π. Following that precedent we assume here also that each phase code element φ_n is restricted to two values, namely 0 or π, with probabilities p and q respectively, such that $p + q = 1$. The φ_n are taken to be a set of independent identically distributed random variables with probability density functions defined as

$$P_\varphi(\varphi) = p\delta(\varphi) + q\delta(\varphi - \pi) \tag{9}$$

where δ denotes Dirac's delta function. This random coding scheme allows us to satisfactorily model the statistics of the encoded (or unsuccessfully decoded) pulses in our proposed CDMA system without restricting ourselves to any particular deterministic code structure. In particular, for purely random sequences ($p = q = 0.5$), the unsuccessfully decoded pulses can be effectively modeled as Gaussian random processes. The assumption of random coding and the resulting Gaussian statistics are expected to be valid for CDMA systems incorporating large numbers of users with long codes [17], [18].

Using (6) the ensemble average of $V(t)$ can be written as

$$\begin{aligned}\langle V(t)\rangle &= \frac{\sqrt{P_0}}{N_0}\sum_{n=-N}^{N}\exp\left\{-in\Omega t)\right\}\langle\exp\left(-i\varphi_n\right)\rangle \\ &= (p-q)V_p(t)\end{aligned} \tag{10}$$

where $\langle\cdot\rangle$ denotes the ensemble average. For $p = q = 0.5$, which corresponds to random encoding, the ensemble average is zero. A more informative result is obtained when one considers the intensity. $I(t)$ can be written as

$$\begin{aligned}I(t) &= \frac{P_0}{N_0^2}\sum_{n=-N}^{N}\sum_{m=-N}^{N} \\ &\quad\cdot\exp\left\{-i\left((n-m)\Omega t + \varphi_n - \varphi_m\right)\right\} \\ &= \frac{P_0}{N_0^2}\left(N_0 + \sum_{n=-N}^{N}\sum_{m\neq n=-N}^{N}\right. \\ &\quad\left.\cdot\exp\left\{-i\left((n-m)\Omega t + \varphi_n - \varphi_m\right)\right\}\right).\end{aligned} \tag{11}$$

Thus the intensity signal $I(t)$ is the sum of a time-independent part P_0/N_0 and a time-varying part which depends upon the phase code. We now calculate the ensemble average $I(t)$ and examine the effect of the phase code

by varying the probabilities p and q. Thus:

$$\langle I(t)\rangle = \frac{P_0}{N_0^2}\left(N_0 + (p-q)^2 \sum_{n=-N}^{N} \sum_{m\neq n=-N}^{N} \cdot \exp\left\{-i(n-m)\Omega t\right\}\right)$$
$$= \langle I(t)\rangle_t + (p-q)^2\left[I_p(t) - \langle I(t)\rangle_t\right]. \quad (12)$$

Here $\langle\cdot\rangle_t$ refers to the time average over one cycle ($T = 2\pi/\Omega$), and $\langle I(t)\rangle_t = P_0/N_0$ is the time average laser intensity. Equation (12) expresses $\langle I(t)\rangle$ as the sum of a low level background with a replica, of amplitude $(p-q)^2$, of the ideal mode-locked pulse $I_p(t)$. For example, if there is no coding, then $p = 0$ and $\langle I(t)\rangle = I_p(t)$. In the case of random coding $p = q = 0.5$ and $\langle I(t)\rangle = \langle I(t)\rangle_t = (P_0/N_0)$. Here the ideal mode-locked pulse $I_p(t)$ disappears, and the ensemble average is equal to the time-average intensity. For other values of p and q, the ensemble average output intensity will have a peak value between that of the uncoded pulse (P_0) and that of a randomly encoded pulse (P_0/N_0). The maximum of the ensemble average occurs at time $t = 0$, and can be written as

$$\langle I(0)\rangle = \frac{P_0}{N_0}\left(1 - (p-q)^2\right) + P_0(p-q)^2. \quad (13)$$

Fig. 5 illustrates six examples that show the effect of different degrees of coding on an ideal band-limited pulse. For these examples, (4) was used to generate the real signal for $P_0 = 1$ and $\Omega = 1$ and for various values of p and N_0. Fig. 5 confirms that for large N_0, $G^2(0)\,I(0)/P_0 \simeq (p-q)^2$, in agreement with (13). These examples illustrate how the ideal mode-locked pulse feature disappears as p and q approach 0.5, leaving behind a weak background intensity. This finding is in close correspondence with results previously obtained for imperfectly mode-locked lasers with nonidentical mode phases [19]–[21].

The time-dependent second-order moment for the intensity signal $I(t)$ can be shown to be

$$\langle I^2(t)\rangle = \left(\frac{P_0^2}{N_0^4}\right)(2N_0(N_0-1))(1-(p-q)^2) + (p-q)^2 I_p^2(t) + \frac{P_0}{N_0^2}\left(1-(p-q)^2\right) \cdot I_p(2t) + \left(\frac{P_0^2}{N_0^4}\right)(p-q)^2\left((p-q)^2-1\right) \cdot \sum\sum\sum \sum_{n\neq m\neq k\neq l} \cdot \exp\left\{i(n-m+k-l)\Omega t\right\}. \quad (14)$$

$I_p(2t)$ represents $I_p(t)$ compressed in time by a factor of 2, but with half the period, so that the peak intensity and the time-average intensity are the same for both. The fourth term in (14), which contains $N_0(N_0-1)(N_0-2)(N_0-3)$ terms, corresponds to mixing among those

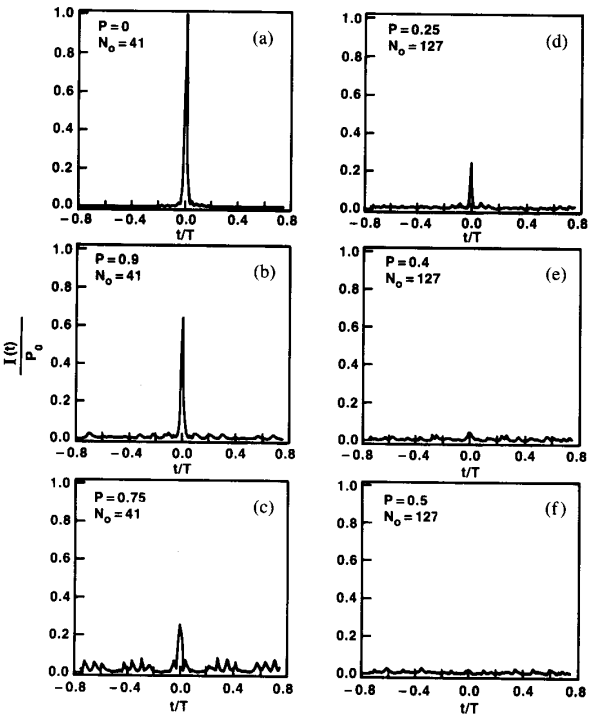

Fig. 5. Intensity profiles of encoded signals generated by spectral phase coding. The phase code consists of N_0 distinct frequency chips. These traces are representative encoded signals produced by using a random number generator to pick the spectral phases. (a) $N_0 = 41$, $p = 0$ (no coding). (b) $N_0 = 41$, $p = 0.9$. (c) $N_0 = 41$, $p = 0.75$. (d) $N_0 = 127$, $p = 0.25$. (e) $N_0 = 127$, $p = 0.4$. (f) $N_0 = 127$, $p = 0.5$.

modes that are different from each other and disappears under random coding, ($p = q = 0.5$) and no coding, ($p = 0$ or $p = 1$). If $p = 0$ (no coding), then $\langle I^2(t)\rangle = I^2(t) = I_p^2(t)$ and for time $t = 0$ we have $I_p^2(0) = P_0^2$. But if $p = q = 0.5$, the second order moment consists of a time-independent term, approximately equal to $2P_0^2/N_0^2$ for $N_0 \gg 1$, and a time-varying term $(P_0/N_0^2)\,I_p(2t)$.

In many applications, such as second harmonic generation measurements of ultrashort pulse durations, we are interested in the time average of the second order moment. For $p = q = 0.5$ and $\langle I_p(2t)\rangle_t = P_0/N_0$, the time average of the second-order moment is equal to

$$\left\langle\left\langle I^2(t)\right\rangle\right\rangle_t = \frac{2P_0^2}{N_0^2}\left(1 - \frac{1}{2N_0}\right) \simeq \frac{2P_0^2}{N_0^2}, \quad \text{for } N_0 \gg 1. \quad (15)$$

The root-mean-square for the randomly encoded signal $I(t)$ is

$$\left(\left\langle\left\langle I^2(t)\right\rangle\right\rangle_t - \langle I(t)\rangle^2\right)^{1/2} = \frac{P_0}{N_0} = \langle I(t)\rangle. \quad (16)$$

The size of fluctuations is equal to the average intensity of the whole laser emission, and its value reduces as the code length increases.

III. The First and Second Degree of Coherence for the Encoded Light Pulse

In this section we calculate the first and second degree of coherence (also known as the field and intensity autocorrelation functions) of the encoded signal.

The ensemble autocorrelation for the encoded electric field $E(t) = V(t) \exp(-i\omega_c t)$, where ω_c is the carrier frequency, can be expressed as

$$\langle E(t)\, E^*(t+\tau)\rangle = \exp(i\omega_c\tau)\left[\frac{\sqrt{P_0}}{N_0} V_p(\tau) + (p-q)^2 \cdot \left[V_p(t)\, V_p(t+\tau) - \frac{\sqrt{P_0}}{N_0} V_p(\tau)\right]\right]. \quad (17)$$

Note that if $\tau = 0$, (17) reduces to (12). The ensemble autocorrelation for the encoded electric field is in general time-dependent, except in the case of random encoding ($p = q = 0.5$). In this case, the time average is equal to the ensemble average. For a randomly encoded pulse, the degree of first-order coherence $g^{(1)}(\tau)$ is given by

$$g^{(1)}(\tau) = \frac{\langle E(t)\, E^*(t+\tau)\rangle}{\langle E(t)\, E^*(t)\rangle} = \exp(i\omega_c\tau)\frac{V_p(\tau)}{\sqrt{P_0}}. \quad (18)$$

We observe that if $\tau = 0$, $|g^{(1)}(0)| = 1$; and if $|\tau| \geq T/N_0 \equiv \tau_c$, where τ_c is the coherence time of the encoded pulse, then for $N_0 >> 1$, $|g^{(1)}(\tau)| \simeq 0$ until the next period T. The shape of the first-order coherence function of an encoded pulse is governed by the ideal mode-locked pulse shape.

The duration of ultrashort light pulses is typically determined by performing intensity autocorrelation measurements [22]; for this reason we examine the intensity autocorrelation function of the encoded signal. The ensemble average intensity autocorrelation can be written as follows:

$$\langle I(t)\, I(t+\tau)\rangle = \frac{P_0^2}{N_0^4}\left(N_0(N_0-2)(1-(p-q)^2)\right) + (p-q)^2 I_p(t)\, I_p(t+\tau) + \frac{P_0}{N_0^2}(1-(p-q)^2) \cdot [I_p(\tau) + I_p(2t+\tau)] + \frac{P_0^2}{N_0^4}(p-q)^2 \cdot ((p-q)^2 - 1) \sum\sum\sum \sum_{n\neq m\neq k\neq l} \cdot \exp\{i[(n-m)\Omega t + (k-l)\Omega(t+\tau)]\}. \quad (19)$$

If $\tau = 0$, (19) reduces to (14) as expected. If $p = 0$, then (19) reduces to

$$\langle I(t)\, I(t+\tau)\rangle = I_p(t)\, I_p(t+\tau) \quad (20)$$

which corresponds to the intensity autocorrelation of the ideal mode-locked pulse. For a randomly encoded signal ($p = 0.5$), (19) reduces to

$$\langle I(t)\, I(t+\tau)\rangle = \frac{P_0^2}{N_0^3}(N_0 - 2) + \frac{P_0}{N_0^2}[I_p(\tau) + I_p(2t+\tau)]. \quad (21)$$

With $\langle I_p(2t+\tau)\rangle_t = P_0/N_0$, the time average of the ensembled autocorrelation function is expressed as

$$\langle\langle I(t)\, I(t+\tau)\rangle\rangle_t = \frac{P_0^2}{N_0^2}\left(1 - \frac{1}{N_0}\right) + \left(\frac{P_0}{N_0^2}\right) I_p(\tau). \quad (22)$$

If $\tau = 0$, then (22) is equal to $(2P_0^2/N_0^2)(1 - (1/2N_0)) \simeq (2P_0^2/N_0^2)$ for $N_0 >> 1$. If $|\tau| \geq \tau_c$, then $I_p(\tau) \simeq 0$ and (22) reduces to $(P_0^2/N_0^2)(1 - (1/N_0)) \simeq (P_0^2/N_0^2)$ for $N_0 >> 1$. Therefore, the peak to background contrast ratio R is given by

$$R \equiv \frac{\langle\langle I(t)^2\rangle\rangle_t}{\langle\langle I(t)\, I(t+\tau)\rangle\rangle_t} = 2, \qquad \text{for } \tau_c \ll |\tau| < T. \quad (23)$$

Furthermore, the degree of the second-order coherence can be expressed as

$$g^{(2)}(\tau) = \frac{\langle\langle I(t)\, I(t+\tau)\rangle\rangle_t}{\langle\langle I(t)^2\rangle\rangle_t} = \frac{1}{2} + \frac{I_p(\tau)}{2P_0} = \frac{1}{2} + \frac{|g^{(1)}(\tau)|^2}{2}. \quad (24)$$

Equation (24) is true for $N_0 >> 1$.

The effect of coding on the intensity autocorrelation is illustrated in Fig. 6, which shows examples of $g^{(2)}(\tau)$ obtained for various code lengths and degrees of coding. The six examples correspond to the six intensity traces shown in Fig. 5 and include the effect of the envelope function $G(t)$ from (4).

If $p = 0$, the intensity autocorrelation function is equal to that of an ideal mode-locked laser pulse with no background [see Fig. 6(a)]. Fig. 6(b) illustrates the intensity autocorrelation for a mode-locked pulse with an encoding parameter of $p = 0.9$. In this case, the intensity autocorrelation has some noisy background due to the coding that was introduced. Note that a strong central spike still exists. For $p = q = 0.5$, the intensity autocorrelation function consists of a "coherence spike" superimposed on a pedestal, with an overall length which is proportional to the duration of the encoded pulse envelope function [see

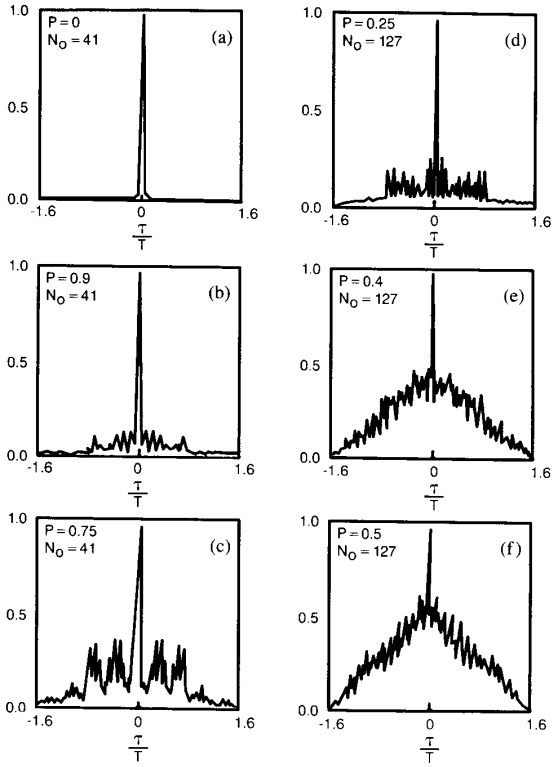

Fig. 6. Intensity autocorrelation traces for the encoded signals shown in Fig. 5. (a) $N_0 = 41$, $p = 0$. (b) $N_0 = 41$, $p = 0.9$. (c) $N_0 = 41$, $p = 0.75$. (d) $N_0 = 127$, $p = 0.25$. (e) $N_0 = 127$, $p = 0.4$. (f) $N_0 = 127$, $p = 0.5$.

Fig. 6(f)]. The coherence spike arises because the encoded signal contains a series of sharp noise spikes with a minimum time duration proportional to the inverse of the source bandwidth. As predicted by (23), the contrast ratio between the height of the coherence spike and the height of the pedestal is 2 : 1. We measured similar intensity autocorrelation in our spectral phase coding experiment, although in the experiment the contrast ratio was somewhat less than 2 : 1. Experimental contrast ratios below 2 : 1 may be an indication that the deterministic codes employed are not perfect examples of random coding. A detailed analysis of pseudonoise bursts generated using a particular set of deterministic codes would have to take into account any structure built into the codes selected and is beyond the scope of this paper.

The intensity autocorrelation shown in Fig. 6(f) is quite similar to intensity autocorrelations corresponding to noise bursts generated from poorly mode-locked lasers [21]–[25]. The presence of a coherence spike on a larger duration pedestal, the 2 : 1 contrast ratio, as well as the relation between the second and first order coherence functions of (24), are expected for any Gaussian noise burst. Thus, random binary spectral phase coding of ultrashort pulses produces pseudonoise signals statistically similar to other forms of random light. However, spectral phase coding of ultrashort pulses generates a *deterministic* random-like signal which can be reconstructed into a coherent ultrashort pulse, as shown by our experiment; therefore, we elect to call such deterministically generated pseudonoise bursts *pseudorandom light* [26].

IV. Probability Density Function for the Encoded Light Pulse

Our discussion of pseudorandom light is not complete without a study of the probability distribution function. We further generalize the expression given in (6) by including two statistically independent random variables, namely t' and η, with probability density functions $P_{t'}(t')$ and $P_\eta(\eta)$, respectively, associated with ambiguities in the transmission time and the initial phase of the encoded light. $P_{t'}(t')$ is defined on the interval $(-T'/2, T'/2)$, where $T' \leq T$, and $P_\eta(\eta)$ is defined on the interval $(-\Pi, \Pi)$, where $\Pi \leq \pi$. This extension is particularly relevant to our analysis of *asynchronous* CDMA systems based on encoding and decoding of ultrashort pulses. Including these random variables, t' and η, (6) can be rewritten

$$V(t - t') = \alpha_x(t - t') - i\alpha_y(t - t'). \tag{25}$$

Here $\alpha_x(t - t')$ and $\alpha_y(t - t')$ are the real and imaginary parts of the complex amplitude $V(t - t')$ and are defined accordingly as

$$\alpha_x(t - t') = \frac{\sqrt{P_0}}{N_0} \sum_{n=-N}^{N} \cos\left(n\Omega(t - t') + \varphi_n + \eta\right) \tag{26}$$

and

$$\alpha_y(t - t') = \frac{\sqrt{P_0}}{N_0} \sum_{n=-N}^{N} \sin\left(n\Omega(t - t') + \varphi_n + \eta\right). \tag{27}$$

The intensity $I(t - t')$ is expressed as $I(t - t') = \alpha_x^2(t - t') + \alpha_y^2(t - t')$. To calculate the probability distribution function for I, it is sufficient to find the joint distribution function $P_{\alpha_x\alpha_y}(\alpha_x, \alpha_y)$. We first consider the simplest case, i.e., $P_{t'}(t') = \delta(t')$ and $P_\eta(\eta) = \delta(\eta)$. Using the method described in [21] or by invoking the central limit theorem, it can be shown that the joint distribution function is, in its most general form, a time varying function and is expressed approximately as

$$P_{\alpha_x\alpha_y}(\alpha_x, \alpha_y, t) = \frac{1}{2\pi\Phi'\Psi'} \exp\left\{-\frac{(\alpha_x - \Upsilon')^2}{2\Phi'^2} - \frac{\alpha_y^2}{2\Psi'^2}\right\} \tag{28}$$

where Υ', Φ'^2 and Ψ'^2 are defined as

$$\Upsilon' = (p - q)V_p(t)$$

$$\Phi'^2 = \left(1 - (p - q)^2\right)\frac{P_0}{2N_0}\left(1 + \frac{V_p(2t)}{\sqrt{P_0}}\right)$$

$$\Psi'^2 = \left(1 - (p - q)^2\right)\frac{P_0}{2N_0}\left(1 - \frac{V_p(2t)}{\sqrt{P_0}}\right).$$

$V_p(2t)$ represents $V_p(t)$ compressed in time by a factor of 2 but with half the period, so that the peak and the time average are the same for both. From (28) we see that the real and imaginary parts of the encoded mode-locked pulse are joint Gaussian random processes.

In the joint probability distribution function, we have kept the code parameters p and q as general as possible. We can illustrate the behavior of the above joint distribution function by evaluating (28) for certain special cases. For example, in the first case of interest, we choose $p = 0$ or $p = 1$ (no coding). In this case then $\Phi'^2 = \Psi'^2 = 0$ and $\Upsilon' = V_p(t)$. Using the fact that

$$\lim_{\sigma \to 0} \frac{1}{\sqrt{2\pi}\sigma} e^{-[(\xi - m)^2/2\sigma^2]} = \delta(\xi - m) \tag{29}$$

where δ denotes the Dirac's delta function, then the probability distribution function reduces to

$$P_{\alpha_x\alpha_y}(\alpha_x, \alpha_y, t) = \delta(\alpha_x - V_p(t))\, \delta(\alpha_y). \tag{30}$$

Thus $\alpha_x(t) = V_p(t)$ and $\alpha_y(t) = 0$.

The second case we evaluate is for $p = q = 0.5$ (random encoding). Then $\Upsilon' = 0$ and $\Phi'^2 = (P_0/2N_0)(1 + (V_p(2t)/\sqrt{P_0}))$ and $\Psi'^2 = (P_0/2N_0)(1 - (V_p(2t)/\sqrt{P_0}))$. It is apparent that the probability distribution function is a time varying function; and in general, pseudonoise bursts generated by spectral phase coding using 0 or π are not stationary processes. We observe that the time dependency of the probability distribution function is due to the variances Φ'^2 and Ψ'^2. We note that the time varying variances for an encoded mode-locked pulse have a mode-locked like pulse shape. Therefore, the major changes as a function of time take place in the vicinity of $|t| \le \tau_c \equiv (2\pi/N_0\Omega)$, for which Φ'^2 takes its maximum value and Ψ'^2 takes its minimum value. For example, at time $t = 0$, $\Phi'^2 = (P_0/N_0)$, $\Psi'^2 = 0$, and (28) reduces to a simple Gaussian distribution function

$$P_{\alpha_x\alpha_y}(\alpha_x, \alpha_y, 0) = \sqrt{\frac{N_0}{2\pi P_0}} \exp\left\{-\frac{N_0\alpha_x^2}{2P_0}\right\} \cdot \delta(\alpha_y). \tag{31}$$

But for $t \ge \tau_c$, $V_p(2t) \simeq 0$ and $\Phi'^2 = \Psi'^2 = (P_0/2N_0)$. Equation (28) then reduces to

$$P_{\alpha_x\alpha_y}(\alpha_x, \alpha_y, t \ge \tau_c) = \frac{N_0}{\pi P_0} \exp\left\{-\frac{N_0\alpha_x^2}{P_0} - \frac{N_0\alpha_y^2}{P_0}\right\}. \tag{32}$$

The above probability function remains independent of time until the next period (at $t = T/2$). The encoded mode-locked pulse with no ambiguity in its transmission time and initial phase is a stationary process for most of its duration, except for the brief period $0 \le |t| \le \tau_c$.

We now consider the general case where t' and η are taken as random variables. For $N_0 >> 1$, the effect of t' and η, in the context of a multiuser interference (CDMA) signal, will not negate the Gaussian approximation. In fact, the Gaussian approximation becomes even more justified [17]. A probability density function can be approximately modeled for this case also and is expressed as follows:

$$P_{\alpha_x\alpha_y}(\alpha_x, \alpha_y, t) = \frac{1}{2\pi\Phi\Psi} \exp\left\{-\frac{(\alpha_x - \Upsilon)^2}{2\Phi^2} - \frac{\alpha_y^2}{2\Psi^2}\right\} \tag{33}$$

where Υ, Φ^2, and Ψ^2 are defined as

$$\Upsilon = (p - q)\langle V_p(t - t')\rangle_{t'}\langle \cos\eta\rangle_\eta$$

$$\Phi^2 = \left(1 - (p - q)^2\right)\frac{P_0}{2N_0} \cdot \left(1 + \frac{\langle \cos 2\eta\rangle_\eta \langle V_p(2(t - t'))\rangle_{t'}}{\sqrt{P_0}}\right) + (p - q)^2\left[\langle I_p(t - t')\rangle_{t'}\langle \cos^2\eta\rangle_\eta - \langle V_p(t - t')\rangle_{t'}^2\langle \cos\eta\rangle_\eta^2\right]$$

$$\Psi^2 = \left(1 - (p - q)^2\right)\frac{P_0}{2N_0} \cdot \left(1 - \frac{\langle \cos 2\eta\rangle_\eta \langle V_p(2(t - t'))\rangle_{t'}}{\sqrt{P_0}}\right) + (p - q)^2\langle I_p(t - t')\rangle_{t'}\langle \sin^2\eta\rangle_\eta.$$

$\langle\cdot\rangle_\eta$ and $\langle\cdot\rangle_{t'}$ are ensemble averages with respect to η and t', respectively. For $P_\eta(\eta) = \delta(\eta)$ and $P_{t'}(t') = \delta(t')$, then (33) reduces to (28). As the last example we consider $p = q = 0.5$, with t' a random variable uniformly distributed on $(-T/2, T/2)$, and η a random variable uniformly distributed on $(-\pi, \pi)$. This corresponds to a randomly encoded pulse with complete ambiguity in its transmission time and initial phase. We find that $\Upsilon = 0$ and

$$\Phi^2 = \Psi^2 = \frac{P_0}{2N_0}. \tag{34}$$

Thus the variances are time-independent and (33) reduces to

$$P_{\alpha_x\alpha_y}(\alpha_x, \alpha_y, t) = \frac{N_0}{\pi P_0} \exp\left\{-\frac{N_0(\alpha_x^2 + \alpha_y^2)}{P_0}\right\}. \tag{35}$$

Equation (35) is true for all time t. Note that, for $p = q = 0.5$, $\eta = 0$, and t' uniformly distributed on the interval $(-T/2, T/2)$ or $p = q = 0.5$, $t' = 0$, and η uniformly distributed on the interval $(-\pi, \pi)$, one achieves a probability density function similar to (35). Therefore, the randomly encoded mode-locked pulse with an unknown time of transmission or initial phase based on our statistical model is a stationary process and can be assumed to be an ergodic process, for which time and ensemble averages for first, second, and higher moments are interchangeable. The probability distribution function defined

in (35) indicates that the real and imaginary parts of the encoded signal are joint Gaussian random variables and are statistically independent. Hence, in this case the intensity signal I has the chi-square probability distribution function and can be shown to be

$$P_I(I) = \begin{cases} \frac{N_0}{P_0} \exp\left\{-\frac{IN_0}{P_0}\right\}, & \text{for } I \geq 0 \\ 0, & \text{for } I < 0. \end{cases} \tag{36}$$

This intensity probability distribution function is typical for all polarized random light [27]–[32]. Hence, we claim that the encoded mode-locked pulse appears to be random light to a receiver with no knowledge of the code, time of transmission, and its initial phase.

V. Performance Analysis

In our system performance evaluation we assume that all users have identical bit rate and signal format and the effects of quantum and thermal noise are neglected. In essence, system performance degrades due to the undesired users' signals that are present in our multiple access channel. Furthermore, we consider the simplest network protocols; it is assumed transmitters and receivers are paired, and communication between each mth (where $1 \leq m \leq M$) transmitter and receiver pair is continuous, where M is the number of users. Fig. 7 depicts a typical coherent ultrashort light pulse CDMA transmitter (encoder) and receiver (decoder) pair. From Fig. 7, our transmitter consists of a band-limited signal source, a data source, and a spectral-phase encoder. The output of the band-limited source, a train of ultrashort pulses of duration τ_c and period T_b, is multiplied (modulated) by a data source that takes on two values, namely "0" or "1," for on–off keying. If the data are "0," then no energy is transmitted and the output of the spectral-phase encoder is zero. On the other hand, if the data are "1," then the ultrashort pulse is sent to the spectral-phase encoder. The spectral-phase encoder adds a determinate phase shift to each spectral component of the electric field of the ultrashort light pulse. This set of spectral phase shifts represent an encoding of the light pulse, hence the term spectral-phase encoder. In the coherent ultrashort light pulse CDMA, the shifted versions of a maximal-length shift register sequence (better known as m-sequences [18]) can be used as the signature sequences, provided that the number of active users on the channel is less than or equal to the length of the m-sequence in use. If the number of users is greater than the code length then the original *Gold* sequences that are in widespread use in multiple-user communication systems can be employed [33]. The result of spectral phase coding is to spread the incident ultrashort pulse into a longer duration lower intensity pseudonoise burst [8], [9]. For an ideal source, the electric field representation for the mth transmitted signal is expressed as

$$E_m(t) = \sum_{j=-\infty}^{\infty} d_j^{(m)} V_m(t - jT_b) \tag{37}$$

where $d^{(m)} = (d_j^{(m)})$ is the mth data sequence that takes on "0" or "1" for every j. $V_m(t - jT_b)$, the encoded unit pulse with a duration equal to T s for every j, is defined as the mth address signal and can be approximately expressed as

$$V_m(t) = \frac{\sqrt{P_0}}{N_0} \sum_{n=-N}^{N} \exp\left(-i(n\Omega t + \varphi_n^{(m)})\right), \quad \text{for } \frac{-T}{2} \leq t \leq \frac{T}{2}. \tag{38}$$

Here P_0 is the peak power of the incident ultrashort pulse, $\varphi_n^{(m)}$ is the nth spectral code element of the mth user's address code, and $N_0 = 2N + 1$ is the total number of code elements. For our analysis we assume that each code element randomly takes on either of two values (0 or π) with equal probability, i.e., we model the codes as binary random sequences. This random coding scheme allows us to satisfactorily model the statistics of the encoded (or unsuccessfully decoded) pulses in our proposed CDMA system without restricting ourselves to any particular deterministic code structure, such as m-sequences or *Gold* sequences. In particular, for purely random sequences, the unsuccessfully decoded pulses were effectively modeled as Gaussian random processes. The assumption of random coding and the resulting Gaussian statistics are expected to be valid for CDMA system incorporating large number of users with long m-sequences or Gold sequences [17]. The encoded pulse is spread over a characteristic time $T = 2\pi/\Omega$, where Ω is the frequency separation between adjacent spectral code elements. Since the duration of the incident ultrashort pulse is $\tau_c \simeq 2\pi/N_0\Omega$, where $N_0\Omega$ is the total bandwidth, we conclude that $T \simeq N_0\tau_c$, i.e., spectral phase coding spreads the original pulse by a factor N_0. In general, the period of the data source (T_b) may be even longer than the encoded pulse duration (T), and we introduce a parameter $K = T_b/T$ which represents this difference (see Fig. 8).

Fig. 7 shows a typical receiver for the coherent ultrashort pulse CDMA communications system. The mth receiver is assumed to be a correlation receiver (matched filter) which is matched to the mth signal; in particular, the mth optical decoder is similar to the mth optical encoder, except that the decoder's spectral-phase code is the complex conjugate of the encoder's spectral-phase code.

The result of the mth encoded signal $E_m(t)$ passing through the kth decoder is designated $E_{mk}(t)$. In an ultrashort pulse CDMA network, in which users send their information asynchronously, the electric field representation of the output of decoder k can be expressed as

$$r(t) = E_{kk}(t) + \sum_{m \neq k} E_{mk}(t - t'_{mk}). \tag{39}$$

$E_{kk}(t)$, representing the desired, successfully decoded signal, is a replica of the original ultrashort pulse with duration τ_c and peak power P_0. The second term of (39) represents the total multiaccess interference signal at the output of decoder k. The unsuccessfully decoded signals

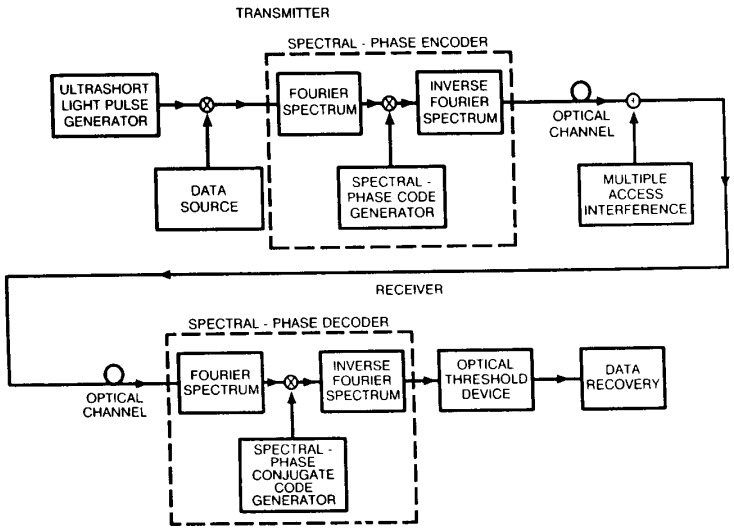

Fig. 7. A typical system representation of an ultrashort pulse CDMA system.

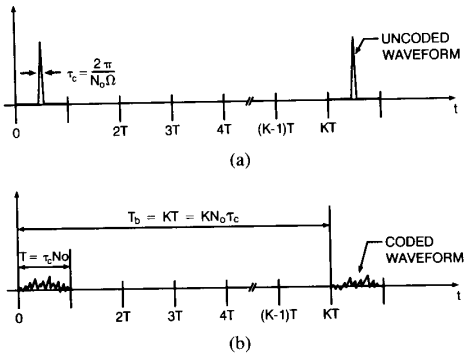

Fig. 8. A schematic timing diagram for coherent ultrashort pulse CDMA. (a) Train of coherent ultrashort pulses. (b) Train of encoded ultrashort pulses.

$E_{mk}(t)$, for $m \neq k$, remain low intensity pseudonoise bursts with average power P_0/N_0 and duration T. With our assumption of random coding, the statistics of the unsuccessfully decoded $E_{mk}(t)$ signals are identical to the statistics of the encoded $E_m(t)$ signal. t'_{mk} denotes the (random) time delay between the arrival of the mth and the kth encoded signals at the decoder k. We assume that $t'_{kk} = 0$, i.e., perfect synchronization is maintained between the desired transmitter and receiver pair.

If we define the intensity signal $I(t) = r(t)\, r^*(t)$, then for on–off keying, the decision can be made by comparing $I(t)$ against a threshold level I_{th}. For our data signal format the desired sampling instants are at $t = 0, T_b, 2T_b \cdots jT_b \cdots$. At these times ($|t - jT_b| \leq \tau_c/2$) the signal $E_{kk}(t)$ is equal to $\sqrt{P_0}$ if $d_j^{(k)} =$ "1" and zero if $d_j^{(k)} =$ "0"; at other times ($|t - jT_b| > \tau_c/2$), $E_{kk}(t)$ is zero independent of $d_j^{(k)}$. The conditional probability densities of the intensity at any of the desired sampling times ($t = jT_b$) are given as follows (see the Appendix):

$$P_I(I/d_0^{(1)} = 0, l) = \frac{N_0}{lP_0}\, e^{-(IN_0/lP_0)} \tag{40}$$

and

$$P_I(I/d_0^{(1)} = 1, l) = \frac{N_0}{lP_0}\, e^{-[N_0(I+P_0)/lP_0]} I_0\left(\frac{2N_0\sqrt{IP_0}}{lP_0}\right) \tag{41}$$

where $I_0(x)$ is the modified Bessel function of the first kind and zeroth order and where $l \geq 1$. For times not coincident with desired sampling times ($|t - jT_b| > \tau_c/2$), the conditional probability density function is given by (40), independent of $d_j^{(k)}$. From (40) and (41) the conditional probability densities are conditioned on the fact that l other users are sending the data "1" at the sampling instant.

In order to calculate the BER we further assume that the receiver detects a "1" if the decoded intensity exceeds the threshold at any time within an interval of duration $\beta\tau_c$ and a "0" otherwise. The threshold could be implemented by using a nonlinear optical device based on an "instantaneous" nonlinearity such as the optical Kerr effect [34], [35]. Electronics in the receiver examine the output of the optical nonlinear device over a duration $\beta\tau_c$, limited by the speed of the electronics. $\beta = 1$ corresponds to the "ideal" thresholder, active only at the instant when the desired data are expected. If we further assume that on–off keying occurs with equal frequency (each with probability $\frac{1}{2}$), then the average probability of error is $\frac{1}{2}(P_{FA} + P_{MD})$, where P_{FA} is the probability that the interference alone crosses the threshold in any of β sampling instants (false alarm), and P_{MD} is the probability that the combination of a transmitted "1" and interference do

not cross the threshold (missed detection). The error rate, obtained from (40) and (41), is as follows (see the Appendix):

$$\text{BER} = \left(\frac{1}{2}\right)\left[\sum_{l=1}^{M-1}\binom{M-1}{l}\left(\frac{1}{2K}\right)^{l}\left(1-\frac{1}{2K}\right)^{M-1-l} \cdot \left(1-\gamma^{\beta-1}(l)\left(\gamma(l)-\rho(l)\right)\right)\right] \quad (42)$$

where

$$\gamma(l) = 1 - e^{-(I_{th}N_0/lP_0)} \quad (43)$$

and

$$\rho(l) = 1 - Q\left(\sqrt{\frac{2N_0}{l}}, \sqrt{\frac{2N_0 I_{\text{th}}}{lP_0}}\right). \quad (44)$$

Here $\gamma(l)$ and $\rho(l)$ can be identified with $1 - P_{FA}$ and P_{MD}, respectively, and $Q(a, b)$ is Marcum's Q function [36], defined as

$$Q(a, b) \equiv \int_b^\infty x \exp\left(\frac{-a^2 - x^2}{2}\right) I_0(ax)\, dx. \quad (45)$$

Fig. 9 shows the BER versus threshold for a CDMA system employing a code length $N_0 = 128$ and $K = 100$, for different number of users (M) and β. For $\beta = 1$ (ideal detection scheme), the minimum errors achievable for $M = 20$ and $M = 100$ are $\simeq 10^{-9}$ and $\simeq 2.8 \times 10^{-7}$, respectively. The minimum error rate is achieved for $I_{\text{th}}/P_0 \simeq \frac{1}{4}$, with the optimum threshold depending only slightly on M. For $\beta = 128$ (not ideal but "practical" detection scheme) the degradation in system performance for $M = 20$ and $M = 100$, compared to the case with $\beta = 1$, is about one order of magnitude. The optimum threshold for this case is slightly greater than the previous case.

Fig. 10 shows the minimum BER versus the number of users (M) for different values of K and N_0, such that the product of KN_0 is fixed at 12800. The minimum BER degrades as the number of users increases. For example, for $\beta = 1$, $K = 25$, and $N_0 = 512$ our system can support up to one hundred users at error rate $\simeq 10^{-10}$ and 500 users at error rate $\simeq 10^{-5}$ provided that the bit rate of each individual user will not exceed $1/\tau_c KN_0$, where τ_c is the duration of an uncoded pulse generated by the ultrashort light pulse generator. For $\tau_c = 80$ fs (0.8 ps), the individual bit rate would be 1 Gbits/s (100 Mbits/s), and the total system transmission capacity would be several hundreds (tens) of gigabits per second.

From Fig. 10 we see that, for a fixed number of users operating at fixed individual bit rates, the system performance improves drastically with increasing the code length (N_0). For example, for $M = 200$ and $\beta = 1$, the minimum error rates achieved for $K = 400$, $N_0 = 32$ and $K = 25$, $N_0 = 512$ are $\simeq 2.0 \times 10^{-4}$ and $\simeq 1.8 \times 10^{-8}$, respectively. The latter BER is four orders of magnitude better than the former. Intuitively, one can argue that by increasing code length, the intensity of the original pulse is spread over longer time and the instantaneous intensity is more effectively reduced, thereby decreasing the probability of false alarm while improving the probability of detection. This example highlights the importance and the dependency of our CDMA system on the code length. From the optics point of view the challenge would be to design a system with a code length as large as possible.

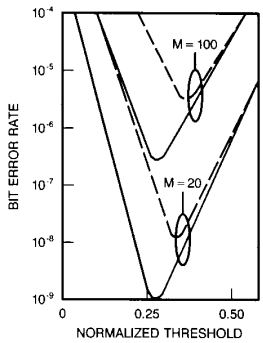

Fig. 9. BER versus normalized threshold (I_{th}/P_0) for code length $N_0 = 128$, $K = 100$. Curves are shown for $M = 20$ and $M = 100$, and for $\beta = 1$ (solid lines) and $\beta = 128$ (dashed lines).

VI. Conclusion

In this paper we studied the temporal and statistical behavior of phase encoded ultrashort light pulses, and examined their performance in the context of a newly proposed optical code-division multiple access communications systems. Under random encoding and unknown time of transmission and initial phase, the encoded pulses were modeled to obey Gaussian statistics and that the intensity probability distribution function is a negative exponential. We calculated the performance of the newly proposed coherent ultrashort light pulse code-division multiple access communications systems as a function of data rate, code length, number of users, and receiver threshold. Furthermore, by increasing the code length (i.e., N_0) the system performance improves drastically; hence more users can be supported. Our calculations give an enticing indication of the potential for ultrashort pulse CDMA to provide hundreds of users with asynchronously multiplexed communications at rates up to the gigabit-per-second range.

Appendix

In this Appendix we will describe the mathematical development of the BER expression derived in Section V. It is convenient to represent the total received signal $r(t)$ as described in (39), during the time interval $(-T/2, +T/2)$. The probability density function $P(I, t)$ of the total received signal $I(t) = r^*(t)\, r(t)$, may be determined from the conditional probability density function $P(I, t/d_0^{(k)}, l)$ of the total received signal, subject to the hypothesis that l users, other than the desired (kth) user, have transmitted binary data "1" during the given interval, by use of the relation

$$P(I, t) = \left\langle \left\langle P(I, t/d_0^{(k)}, l)\right\rangle_l \right\rangle_{d_0^{(k)}}. \quad (A1)$$

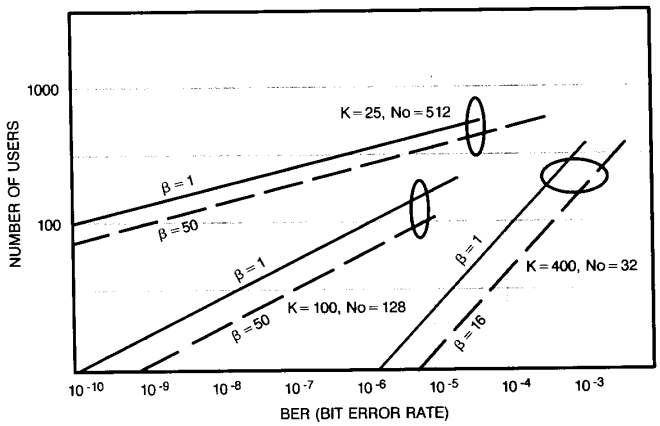

Fig. 10. BER versus number of users (M) for different values of K and N_0, such that the product KN_0 is fixed at 12 800. (a) $K = 400$, $N_0 = 32$, and $\beta = 1, 16$. (b) $K = 100$, $N_0 = 128$, and $\beta = 1, 50$. (c) $K = 25$, $N_0 = 512$, and $\beta = 1, 50$.

Here l is a random variable with a binomial distribution

$$P(l) = \binom{M-1}{l} \zeta^l (1-\zeta)^{M-1-l} \qquad \text{(A2)}$$

where $\zeta = 1/2K$, and $K = T_b/T$ was defined in Section V.

To calculate the conditional probability distribution function $P(I, t/d_0^{(k)}, l)$, it is sufficient to find the conditional joint distribution function $P_{r_x r_y}(r_x, r_y, t/d_0^{(k)}, l)$, where r_x and r_y are the real and imaginary parts of the received signal $r(t)$, defined as in (39). The real and imaginary parts of the received signal are modeled as jointly Gaussian and from (35) the conditional joint distribution function can be expressed as

$$P_{r_x r_y}(r_x, r_y, t/d_0^{(k)}, l) = \frac{1}{2\pi l\sigma^2} \exp\left\{-\frac{1}{2}\frac{\left(r_x - d_0^{(k)} V_p(t)\right)^2 + r_y^2}{l\sigma^2}\right\}. \qquad \text{(A3)}$$

Here $\sigma^2 = P_0/2N_0$. Note that for $l = 0$, which occurs with probability $(1-\zeta)^{M-1}$, then the joint distribution function reduces to

$$P_{r_x r_y}(r_x, r_y, t/d_0^{(k)}, l = 0) = \delta\left(r_x - d_0^{(k)} V_p(t)\right) \delta(r_y) \qquad \text{(A4)}$$

and the conditional probability density function $P(I, t/d_0^{(k)}, l = 0)$ can be expressed as

$$P(I, t/d_0^{(k)}, l = 0) = \delta\left(I - d_0^{(k)} I_p(t)\right). \qquad \text{(A5)}$$

From the above equation if $d_0^{(k)} = 0$ then $I = 0$ (with probability one), and if $d_0^{(k)} = 1$ then $I = I_p(t)$ (with probability one), for $-T/2 \le t \le T/2$.

From (A3) the conditional probability density function for $l \ge 1$ is expressed as

$$P(I, t/d_0^{(k)}, l) = \frac{N_0}{lP_0} e^{-[N_0(I + d_0^{(k)} I_p(t))/lP_0]} \cdot I_0\left(\frac{2N_0\sqrt{Id_0^{(k)} I_p(t)}}{lP_0}\right) \qquad \text{(A6)}$$

where $I_0(x)$ is the modified Bessel function of the first kind and zeroth order. Note that the conditional probability density function is derived as a function of time and the data $d_0^{(k)}$. For example, for $d_0^{(k)} = 0$, which we assume it occurs with probability $1/2$ for memoryless sources, then the above density function reduces to (40). On the other hand at $t = 0$ and $d_0^{(k)} = 1$, then the above density function reduces to (41). For $d_0^{(k)} = 1$ and $|t| \ge \tau_c/2$, then $I_p(t) \simeq 0$, then the distribution function reduces to (40), since $I_0(x) \simeq 1$ for $x << 1$ in (A6).

From (A2) and (A6) the probability density function $P(I, t/d_0^{(k)})$ can be expressed as

$$P(I, t/d_0^{(k)}) = (1-\zeta)^{M-1} \delta\left(I - d_0^{(k)} I_p(t)\right) + \sum_{l=1}^{M-1} P(l)\, p(I, t/d_0^{(k)}, l). \qquad \text{(A7)}$$

From (A1) and (A7) the unconditional probability density function is expressed as

$$P(I, t) = \tfrac{1}{2}\left[P(I, t/d_0^{(k)} = 0) + P(I, t/d_0^{(k)} = 1)\right]. \qquad \text{(A8)}$$

To determine the BER, we first determine the bit-error-rate conditioned on l [i.e., BER(l)], and use the relation BER $= \langle \text{BER}(l) \rangle_l$ to calculate the average system per-

formance. For our data signal format the desired sampling instant is at $t = 0$. At this time the signal $I_p(t = 0) = P_0$. Furthermore we assume ideal detection scheme; $\beta = 1$ in (42); then

$$\begin{aligned} \mathrm{BER}(l) &= P_r(I \geq I_{\mathrm{th}}/d_0^{(k)} = 0, l)\, P_r(d_0^{(k)} = 0) \\ &\quad + P_r(I < I_{\mathrm{th}}/d_0^{(k)} = 1, l)\, P_r(d_0^{(k)} = 1) \\ &= \tfrac{1}{2}[P_{FA}(l) + P_{MD}(l)]. \end{aligned} \tag{A9}$$

Here $P_{FA}(l)$ and $P_{MD}(l)$ correspond to the probabilities of *false alarm* and *miss detection*. Using (40), (41), (A2), and (A9), then one achieves the BER as described in (42) for $\beta = 1$.

We now discuss the case where $\beta \geq 1$. In order to calculate the BER we postulate that the receiver detects a "1" if the decoded intensity exceeds the threshold at any time within an interval of duration $\beta\tau_c$ and a "0" otherwise. Under the hypothesis that $d_0^{(k)} = 0$, then

$$\begin{aligned} P_{FA}(l) &= P_r(I_1 \geq I_{\mathrm{th}}/l) + P_r(I_1 < I_{\mathrm{th}}/l) \\ &\quad \cdot P_r(I_2 \geq I_{\mathrm{th}}/l) + P_r(I_1 < I_{\mathrm{th}}, I_2 < I_{\mathrm{th}}/l) \\ &\quad \cdot P_r(I_3 \geq I_{\mathrm{th}}/l) + \cdots \\ &\quad + P_r(I_1 < I_{\mathrm{th}}, I_2 < I_{\mathrm{th}}, \cdots, I_{\beta-1} < I_{\mathrm{th}}/l) \\ &\quad \cdot P_r(I_\beta \geq I_{\mathrm{th}}/l). \end{aligned} \tag{A10}$$

Here I_i, for $1 \leq i \leq \beta$, is the value of the instantaneous intensity at the ith coherence cell within the interval $(-(\beta\tau_c/2), \beta\tau_c/2)$. For $\gamma(l) = P_r(I_i < I_{\mathrm{th}}/l)$, where $\gamma(l)$ is defined as in (43), and since the instantaneous intensities within each coherence cell are statistically independent, then the conditional probability of false alarm $P_{FA}(l)$ can be expressed as

$$P_{FA}(l) = 1 - \gamma^{\beta}(l). \tag{A11}$$

Similarly, using (A6) the probability of detection or probability of missed detection $P_{MD}(l) = 1 - P_D(l)$, can be expressed as

$$P_{MD}(l) = \gamma^{\beta-1}(l)\, \rho(l) \tag{A12}$$

where $\rho(l)$ is defined as in (44). Using (A2), (A11), and (A12), then $\mathrm{BER} = \frac{1}{2}[\langle P_{FA}(l) \rangle_l + \langle P_{MD}(l) \rangle_l] = \frac{1}{2}[P_{FA} + P_{MD}]$, and it is expressed as in (42).

Acknowledgment

The authors gratefully acknowledge helpful discussions and full support of this work by C. A. Brackett and P. W. Smith. The authors would like to thank E. Arthurs and F. A. Descloux for number of fruitful discussions. They also acknowledge the superb technical assistance of E. M. Kirschner and D. E. Leaird, and thank the reviewers for their careful reading and remarks as well.

References

[1] "Optical multiaccess networks," *IEEE Network*, vol. 3, no. 2, Mar. 1989.
[2] J. A. Salehi, "Code division multiple-access techniques in optical fiber networks—Part I: Fundamental principles," *IEEE Trans. Commun.*, vol. 37, no. 8, pp. 824–833, Aug. 1989.
[3] J. A. Salehi and C. A. Brackett, "Code division multiple-access techniques in optical fiber networks—Part II: Systems performance analysis," *IEEE Trans. Commun.*, vol. 37, no. 8, pp. 834–842, Aug. 1989.
[4] G. Vannucci and S. Yang, "Experimental spreading and despreading of the optical spectrum," *IEEE Trans. Commun.*, vol. 37, no. 7, pp. 777–780, July 1989.
[5] J. Y. Hui, "Pattern code modulation and optical decoding—A novel code-division multiplexing techniques for multifiber network," *IEEE J. Selected Areas Commun.*, vol. SAC-3, pp. 916–927, 1985.
[6] P. R. Prucnal, M. A. Santoro, and T. R. Fan, "Spread spectrum fiber-optic local area network using optical processing," *J. Lightwave Technol.*, vol. LT-4, pp. 547, 1986.
[7] G. J. Foschini and G. Vannucci, "Using spread-spectrum in a high capacity fiber-optic local area network," *J. Lightwave Technol.*, vol. 6, no. 3, p. 370, 1988.
[8] A. M. Weiner, J. P. Heritage, and J. A. Salehi, "Frequency domain coding of femtosecond pulses for spread-spectrum communications," in *Proc. Conf. Lasers Electrooptics* (Baltimore, MD), Apr. 1987, pp. 294–296, postdeadline pap.
[9] A. M. Weiner, J. P. Heritage, and J. A. Salehi, "Encoding and decoding of femtosecond pulses," *Opt. Lett.*, vol. 13, no. 4, pp. 300–302, Apr. 1988.
[10] R. Skaug and J. F. Hjelmstad, *Spread Spectrum in Communications*. London, U.K.: Peregrinus, 1985.
[11] J. P. Heritage, A. M. Weiner, and R. N. Thurston, "Picosecond pulse shaping by spectral phase and amplitude manipulation," *Opt. Lett.*, vol. 10, p. 609, 1985.
[12] A. M. Weiner, J. P. Heritage, and R. N. Thurston, "Synthesis of phase coherent, picosecond optical square pulses," *Opt. Lett.*, vol. 11, p. 153, 1986.
[13] R. N. Thurston, J. P. Heritage, A. M. Weiner, and W. J. Tomlinson, "Analysis of picosecond pulse shape synthesis by spectral masking in a grating pulse compressor," *IEEE J. Quantum Electron.*, vol. QE-22, p. 682, 1986.
[14] A. M. Weiner, J. P. Heritage, and E. M. Kirschner, "High-resolution femtosecond pulse shaping," *J. Opt. Soc. Amer. B*, vol. 5, pp. 1563–1572, Aug. 1988.
[15] A. Frenkel, J. P. Heritage, and M. Stern, "Compensation of dispersion in optical fibers for the 1.3–1.6 μm region with a grating and telescope," *IEEE J. Quantum. Electron.*, vol. 25, no. 9, pp. 1981–1984, Sept. 1989.
[16] M. Stern, J. P. Heritage, and R. N. Thurston, unpublished.
[17] C. L. Weber, G. K. Huth, and B. H. Batson, "Performance considerations of code division multiple-access systems," *IEEE Trans. Veh. Technol.*, vol. VT-30, no. 1, pp. 3–10, Feb. 1981.
[18] D. V. Sarwate and M. B. Pursley, "Crosscorrelation properties of pseudorandom and related sequences," *Proc. IEEE*, vol. 68, no. 5, pp. 593–619, May 1980.
[19] A. A. Grutter, R. Dandliker, and H. P. Weber, "The output intensity of a nonideally mode-locked laser," *Z. Agnew. Math. Phys.*, vol. 20, pp. 574–577, July 1969.
[20] A. A. Grutter, H. P. Weber, and R. Dandliker, "Imperfectly mode-locked laser emission and its effects on nonlinear optics," *Phys. Rev.*, vol. 185, pp. 629–643, Sept. 1969.
[21] R. Dandliker, A. A. Grutter, and H. P. Weber, "Statistical amplitude and phase variations in mode-locked lasers," *IEEE J. Quantum Electron.*, vol. QE-6, no. 11, pp. 687–693, Nov. 1970.
[22] E. P. Ippen and C. V. Shank, *Ultrashort Light Pulses*, S. L. Shapiro, Ed. New York: Springer-Verlag, 1977.
[23] M. A. Duguay, J. W. Hansen, and S. L. Shapiro, "Study of Nd:Glass laser radiation," *IEEE J. Quantum Electron.*, vol. QE-6, no. 11, pp. 725–743, Nov. 1970.
[24] H. A. Pike and M. Hercher, "Basis for picosecond structure in mode-locked laser pulses," *J. Appl. Phys.*, vol. 41, no. 11, pp. 4562–4565, Oct. 1970.
[25] H. A. Haus, C. V. Shank, and E. P. Ippen, "Shape of passively mode-locked laser pulses," *Opt. Commun.*, vol. 15, no. 1, pp. 29–31, Sept. 1975.
[26] J. A. Salehi, "Pseudorandom light from a mode-locked laser," *Opt. Lett.*, vol. 14, Feb. 1989.
[27] L. Mandel, "Fluctuations of photon beams and their correlations," *Proc. Phys. Soc.*, vol. 72, pp. 1037–1048, 1958.
[28] L. Mandel, "Fluctuations of photon beams: The distribution of the photoelectrons," *Proc. Phys. Soc.*, vol. 74, pp. 233–243, 1959.

[29] L. Mandel and E. Wolf, "Coherence properties of optical fields," in *Rev. Mod. Phys.*, vol. 37, no. 2, pp. 231–287, Apr. 1965.
[30] R. Loudon, *The Quantum Theory of Light*, 2nd ed. Oxford, U.K.: Oxford Univ. Press, 1983.
[31] B. Saleh, *Photoelectron Statistics*. New York: Springer-Verlag, 1978.
[32] J. W. Goodman, *Statistical Optics*. New York: Wiley, 1985.
[33] R. Gold, "Optimal binary sequences for spread spectrum multiplexing," *IEEE Trans. Inform. Theory*, vol. IT-13, pp. 619–621, Oct. 1967.
[34] S. M. Jensen, *IEEE J. Quantum Electron.*, vol. QE-18, p. 1580, 1982.
[35] S. R. Friberg, A. M. Weiner, Y. Silberberg, B. G. Sfez, and P. W. Smith, "Femtosecond switching in a dual-core-fiber nonlinear coupler," *Opt. Lett.*, vol. 13, pp. 904–906, Oct. 1988.
[36] J. I. Marcum, "A statistical theory of target detection by pulsed radar," *Trans. IRE Prof. Group Inform. Theory*, vol. IT-6, no. 2, pp. 59–144, Apr. 1960.

*

Jawad A. Salehi (S'80–M'84) was born in Kazemain, Iraq, on December 22, 1956. He received the B.S. degree in electrical engineering from University of California at Irvine in 1979 and the M.S. and Ph.D. degrees in electrical engineering from University of Southern California in 1980 and 1984, respectively.

From 1981 to 1984 he was a full-time Research Assistant at Communications Sciences Institute at USC engaged in research in the area of spread spectrum code-division multiple access (CDMA) networks. Since 1984 he has been a Member of the Technical Staff in the Applied Research Area at Bell Communications Research (Bellcore), Morristown, NJ. His current research interests are in the areas of communication theory, optical signal processing techniques for optical networks, in particular, fiber-optic CDMA and ultrashort light pulse CDMA, optical sequences, and optical neuromorphic networks.

Dr. Salehi is a member of Optical Society of America and he is a recipient of the Bellcore's Award of Excellence. He helped, as a member of the organizing committee, to organize the first and the second IEEE Conference on Neural Information Processing Systems—Natural and Synthetic, November 1987 and November 1988, Denver, CO.

*

Andrew M. Weiner was born in Boston, MA, on July 25, 1958. He received the S.B., S.M., and Sc.D. degrees in electrical engineering from M.I.T. in 1979, 1981 and 1984, respectively. From 1979 through 1984, he was a Fannie and John Hertz Foundation Graduate Fellow. His doctoral thesis, for which he was awarded a 1984 Fannie and John Hertz Foundation Doctoral Thesis Prize, dealt with femtosecond pulse compression and measurement of femtosecond dephasing in condensed matter.

In 1984 he joined Bellcore in Red Bank, NJ, where he has conducted research on shaping of ultrashort optical pulses, optical probing of picosecond electronics, all-optical switching, and ultrafast nonlinear optics in fibers. His current research interests center on applications of pulse shaping to femtosecond spectroscopy, dark soliton propagation in fibers, and ultrahigh speed photonic switching. He is presently District Manager of Ultrafast Optics and Optical Signal Processing Research.

Dr. Weiner is an Associate Editor of the IEEE JOURNAL OF QUANTUM ELECTRONICS, and in 1988–1989 he was an IEEE Lasers and Electrooptics Society Traveling Lecturer. He has served on the program committee of several conferences and was vice-chairman of the 1989 Gordon Conference on Nonlinear Optics and Lasers.

*

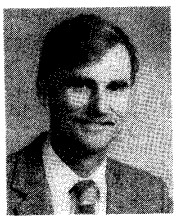

Jonathan P. Heritage (S'74–M'75–SM'89) received the B.S. degree in electrical engineering from the University of California, Berkeley, CA, in 1967, the M.S. degree in physics from San Diego State University, in 1971, and the Ph.D. degree in electrical engineering from the University of California, Berkeley, in 1975.

From 1975 to 1976, he was with the Physics Department of the Technical University of Munich, Federal Republic of Germany, as a Postdoctoral Fellow of the Alexander von Humbouldt Stiftung, where his studies concentrated on picosecond lifetime measurements in organic compounds. In 1976 he joined the staff of Bell Laboratories, Holmdel, NJ, where he was a Member of Technical Staff. On January 1, 1984 he joined Bellcore, Red Bank, NJ, in the Solid State Science and Technology Research Laboratory, where he is a Distinguished Member of Professional Staff. His research has led to contributions to the development of high-sensitivity spectroscopy using synchronized tunable picosecond lasers, vibrational stimulated Raman spectroscopy of monolayers, and surface enhanced nonlinear optics. Subsequently he investigated rapid carrier recombination in compound and layered semiconductors. His recent work includes studies of the dynamic Stark effect in reduced dimensionality semiconductor systems and the phonon mediated Stark effect in Polydiacetylene. He also has investigated fiber and grating compression in the presence of efficient stimulated Raman conversion. His present interests are in the technique of femtosecond pulse shaping and its application to spectroscopy, fiber propagation, and ultra-high rate fiber optic communications.

Dr. Heritage is a Fellow of the Optical Society of America and a member of the American Physical Society. He is an Associate Editor of IEEE PHOTONICS TECHNOLOGY LETTERS and a past Associate Editor of the IEEE JOURNAL OF QUANTUM ELECTRONICS.